



Isolation and Structural Characterization of a Mackay 55-Metal-Atom Two-Shell Icosahedron of Pseudo- I_h Symmetry, $\text{Pd}_{55}\text{L}_{12}(\mu_3\text{-CO})_{20}$ ($\text{L} = \text{PR}_3$, $\text{R} = \text{Isopropyl}$): Comparative Analysis with Interior Two-Shell Icosahedral Geometries in Capped Three-Shell Pd_{145} , Pt-Centered Four-Shell Pd-Pt M_{165} , and Four-Shell Au_{133} Nanoclusters

Jeremiah D. Erickson,^{†,‡} Evgueni G. Mednikov,[†] Sergei A. Ivanov,[§] and Lawrence F. Dahl^{*,†}[†]Department of Chemistry, University of Wisconsin—Madison, Madison, Wisconsin 53706, United States[§]Center for Integrated Nanotechnologies, Los Alamos National Laboratory, Los Alamos, New Mexico 87545, United States

Supporting Information

ABSTRACT: We present the first successful isolation and crystallographic characterization of a Mackay 55-metal-atom two-shell icosahedron, $\text{Pd}_{55}\text{L}_{12}(\mu_3\text{-CO})_{20}$ ($\text{L} = \text{PPR}_3$) (1). Its two-shell icosahedron of pseudo- I_h symmetry (without isopropyl substituents) enables a structural/bonding comparison with *interior* 55-metal-atom two-shell icosahedral geometries observed within the multi-shell capped 145-metal-atom three-shell $\text{Pd}_{145}(\text{CO})_{72}(\text{PEt}_3)_{30}$ and 165-metal-atom four-shell Pt-centered ($\mu_{12}\text{-Pt}$)- $\text{Pd}_{164-x}\text{Pt}_x(\text{CO})_{72}(\text{PPh}_3)_{20}$ ($x \approx 7$) nanoclusters, and within the recently reported four-shell $\text{Au}_{133}(\text{SC}_6\text{H}_4\text{-}i\text{-Bu}^t)_{52}$ nanocluster. DFT calculations carried out on a $\text{Pd}_{55}(\text{CO})_{20}(\text{PH}_3)_{12}$ model analogue, with triisopropyl phosphine substituents replaced by H atoms, revealed a positive +0.84 e charge for the entire Pd_{55} core, with a highly positive second-shell Pd_{42} surface of +1.93 e .

In 1962, Mackay¹ reported that a close-packed assembly of equal-sized spheres can form concentric shells of either regular icosahedra or cuboctahedra; the second icosahedral or cuboctahedral shell of spheres, packed over the first shell (i.e., the centered 13-atom icosahedron or cuboctahedron), consists of 42 spheres. In general, either the icosahedral or cuboctahedral n th shell is composed of $(10n^2+2)$ spheres. A regular icosahedron of I_h symmetry is one of five Platonic solids with 12 identical vertices, 20 equivalent triangular faces, and 30 edges; a regular cuboctahedron of O_h symmetry is one of 13 Archimedean solids containing 12 identical vertices, 8 triangular and 6 square faces, and 30 edges.^{2–4} Figure S1 in the Supporting Information shows the close geometrical relationship between the icosahedron and the cuboctahedron; both structures can exist as concentric two-shell systems, with the second shell being either a 42-atom ν_2 icosahedron or ν_2 cuboctahedron (where ν_n denotes $(n+1)$ atoms along each edge).

Syntheses of extremely air-sensitive powder samples of several two-shell metal-atom clusters $\text{M}_{55}\text{L}_{12}\text{Cl}_x$ with 12 bulky phosphine or arsine ligands L and with either 6 or 20 Cl ligands were first reported 30 years ago by Schmid et al.,⁵ involving reductions of ML_nCl_x complexes with diborane (B_2H_6) in organic solvents: reported formulas are $\text{M}_{55}(\text{PPh}_3)_{12}\text{Cl}_6$ ($\text{M} =$

Au , Rh), $\text{M}_{55}\{\text{P}(t\text{-Bu})_3\}_{12}\text{Cl}_{20}$ ($\text{M} = \text{Rh}$, Ru), and $\text{Pt}_{55}\{\text{As}(t\text{-Bu})_3\}_{12}\text{Cl}_{20}$. Because efforts to obtain crystals for structural determinations were not successful, these clusters were characterized indirectly by spectroscopic methods, molecular weight determinations, elemental analyses, and high-resolution transmission electron microscopy (HRTEM). Schmid et al.⁵ proposed (Figure S2) that these clusters were “understandable” only if they had *cuboctahedral* metal architectures.

The 55-metal-atom two-shell cluster contains a “magic number” of atoms (i.e., the number of atoms in full-shell cluster systems that are presumed to be especially stable because of their complete outer geometry). This number was first deduced from mass spectrometric intensities for “full” Xe clusters nucleated in the gas phase.^{6a} The composite 55-atom two-shell icosahedron has been designated^{6b} as a two-shell Mackay icosahedron (MI), in which 20 identical (but slightly distorted) ν_2 tetrahedra that share a common central vertex (containing the centered atom) are connected to one another through adjacent shared tetrahedral faces.

In 2002, Kuo⁷ emphasized the tremendous impact of Mackay’s findings¹ on the fields of nanoparticles, intermetallic clusters, and quasicrystals. Kuo⁷ stressed the importance of Mackay’s concept of hierarchic icosahedral structures resulting from the presence of a stacking fault in *fcc* packing of successive triangular faces of the icosahedral shells. He also pointed out that the so-called two-shell MI had been suggested (but not proven)^{8,9} to be a possible structural motif for Al-M icosahedral quasi-crystals ($\text{M} = \text{Mn}$, Fe)^{10,11} that subsequently were considered to be Mackay-type quasi-crystals¹² of 5-fold symmetry.

Our work at UW-Madison over the past 20 years¹³ has established that zerovalent Pd forms an extraordinary diversity of nanosized CO/ PR_3 -ligated icosahedral and *ccp/hcp*-based (homo/hetero) Pd_n clusters; these include two structurally related multi-shell icosahedral clusters containing 55 *interior* metal atoms within the first two shells that conform to the icosahedral Mackay model: namely, a three-shell 145-metal-atom $\text{Pd}_{145}(\text{CO})_x(\text{PEt}_3)_{30}$ ($x \approx 60$) cluster (2)^{14a} and a Pd-Pt four-shell 165-metal-atom ($\mu_{12}\text{-Pt}$)- $\text{Pd}_{164-x}\text{Pt}_x(\text{CO})_{72}(\text{PPh}_3)_{20}$ ($x \approx 7$) cluster (3).^{14b} The geometries of the two-shell Mackay

Received: December 14, 2015

Published: January 21, 2016

icosahedra within these multi-shell 145- and 165-metal-atom clusters are virtually identical. *Ab initio* calculations¹⁵ of the total energies and relaxed geometries for “bare” gas-phase Pd₅₅, Ru₅₅, and Ag₅₅ clusters revealed an energetic preference for the two-shell icosahedron over the two-shell cuboctahedron (*fcc*).

Mackay¹ proposed that formation of the third shell of a *normal* icosahedron required the arrangement of 20, 10-atom triangles (each corresponding to a ν_3 equilateral triangle) above the 20 ν_2 equilateral triangular faces to give a 147-atom regular three-shell icosahedron, designated as an edge-capping/vertex¹⁶ or Mackay overlayer.¹⁷ However, shell 3 in both **2** and **3** has only 60 Pd atoms, involving three Pd atoms located at the three equivalent internal sites of the 6-atom ν_2 triangular face of each of the 20 tetrahedra in the second shell to give a 60-atom polyhedron.¹⁸ Because shell 3 only has 60 atoms (instead of $10(3)^2 + 2 = 92$ atoms for the normal Mackay vertex-(edge-shared) shell growth), the three shells in both **2** and **3** possess 115 instead of 147 atoms. This *twin* atomic arrangement for shell 3, which has also been termed a face-capping vertex¹⁶ or icosahedral *anti*-Mackay third shell,¹⁷ gives rise to a semiregular Archimedean polyhedron of 60 equivalent capping vertices (named a rhombicosidodecahedron),^{2–4} which is a stereoisomer of the truncated icosahedral Buckminsterfullerene C₆₀ molecule (buckyball),¹⁹ another icosahedral Archimedean polyhedron of *I_h* symmetry. Figure S3 displays side/top views of the *composite* four-shell 165-metal-atom architecture and Figure S4 its *separate* concentric four-shell anatomies in the Pt-centered Pt_xPd_{165-x} icosahedral core ($x \approx 8$) of **3**.

Two recent independent stereochemical investigations^{20,21} of different crystalline polymorphs of Au₁₃₃(SC₆H₄-*p*-Bu^t)₅₂ produced virtually identical results: an isostructural *interior* 55-metal-atom two-shell MI with shell 3 in an *anti*-Mackay atom arrangement comprised of 52 Au atoms in the rhombicosidodecahedral polyhedron (instead of the “filled” 60 atoms observed for 145 Pd and 165 (Pd-Pt) atom structures). The remaining outermost 26 Au(I) atoms in shell 4 are part of 26 thiolate (RS-Au-SR) staples (R = C₆H₄-*p*-Bu^t) that sterically/electronically stabilize the Au₁₃₃ nanocluster.

Herein we report the first isolation of a crystalline two-shell Mackay icosahedral cluster, Pd₅₅L₁₂(μ_3 -CO)₂₀ with L = P(*i*-Pr)₃ (**1**). The structure was determined from crystallographic analyses of two different solvated crystals (*vide infra*). Of particular significance is its much *greater* stabilization relative to the 55-metal-atom non-crystalline M₅₅L₁₂Cl_x ($x = 6$ or 20) clusters previously reported by Schmid et al.⁵ The especially bulky triisopropylphosphine (P(*i*-Pr)₃) ligands in **1**, furnished by the prepared Pd₁₀(CO)₁₂{P(*i*-Pr)₃}₆ precursor (**S1**), were chosen in the hope (successfully realized) that the resulting metal-surface arrangement would sterically prevent further sequential conversions of the Pd₅₅ cluster (**1**) into other Pd_n clusters.

Figure 1 shows the molecular structure of **1** obtained from complete CCD X-ray diffractometry investigations at 100 K of (*i*-Pr)₂O-solvated crystals **1a**²² and THF-solvated crystals **1b**.²³ Table S1 shows that all of the corresponding mean Pd-Pd distances of **1** in **1a** and **1b** are within 0.01 Å of each other; hence, only those of **1** from **1a** are utilized in the structural comparison with **2** and **3**. Figure 2 gives comparative views of the two-shell geometry of **1** and those of the four-shell 165-metal-atom (μ_{12} -Pt)Pd_{164-x}Pt_x nanocluster ($x \approx 7$) (**3**) and of the capped three-shell Pd₁₄₅(PEt₃)₃₀ cluster (**2**). Table 1 presents a comparison of mean metal-metal distances in **1** for the six different types of metal-metal distances labeled under pseudo-*I_h* symmetry with those for shells 1 and 2 in both **2** and **3** and also with those

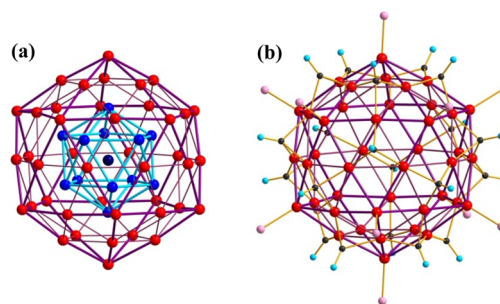


Figure 1. View of Pd₅₅L₁₂(μ_3 -CO)₂₀ (L = PR₃; R = isopropyl) (**1**) displaying (a) “Matryoshka doll sequence” of central Pd atom encapsulated by the Pd₁₂ icosahedron in shell 1, which in turn is encapsulated by the Pd₄₂ icosahedron in shell 2. The 42 atoms in the second ν_2 icosahedral shell (where ν_n denotes $(n+1)$ equally spaced atoms along each edge) may be generated by the superposition of a 6-atom ν_2 triangular Pd(C)₃Pd(D)₃ face onto each ν_1 triangular Pd(B)₃ face of the inner centered 13-atom icosahedron. This two-shell icosahedron of 55 metal atoms (that ideally conforms to *I_h* (2/*m*35) symmetry) is the first crystallographically documented example of the Mackay icosahedron. (b) An identical orientation of 42 surface atoms in the second icosahedral shell of Pd₅₅(PR₃)₁₂(μ_3 -CO)₂₀ showing (1) coordination of 12 Pd(C) vertices along six 5-fold axes with 12 PR₃ ligands (without bulky isopropyl R substituents) and (2) linkage of 20 triply bridging CO ligands with the inner Pd(D)₃ triangle of 20, 6-atom ν_2 triangular Pd(C)₃Pd(D)₃ faces.

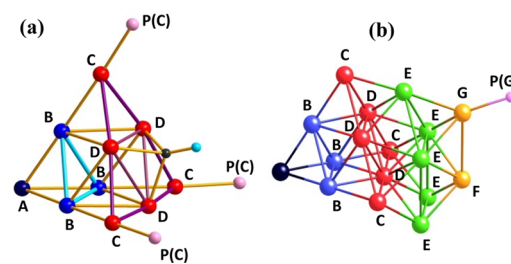


Figure 2. Comparative views of the multi-shell metal anatomies along a 3-fold axis with analogous designated atom-labeling under pseudo-*I_h* symmetry (Table 1) for (a) the two-shell 55-metal-atom core along with a triply bridging (μ_3 -CO) ligand and attached P(C) atoms in the Pd₅₅{P(*i*-Pr)₃}₁₂ cluster (**1**) and (b) the four-shell 165-metal-atom (μ_{12} -Pt)Pd_{164-x}Pt_x(PPh₃)₂₀ cluster ($x \approx 7$) (**3**) and capped three-shell Pd₁₄₅(PEt₃)₃₀ cluster (**2**). The similarly oriented 3-fold axis in both (a) and (b) passes through the central M(A) atom, the midpoint of the Pd(B)₃ triangle in shell 1, the midpoint of the inner Pd(D)₃ triangle in shell 2, and its attached (μ_3 -CO) ligand in (a) for **1** and the midpoint of the Pd(E)₃ triangle in shell 3 and its attached Pd(G) and phosphine P(G) atoms in (b) for **3**. The structurally related 145-metal-atom structure **2** can be derived from the 165-metal-atom cluster **3** in (b) by the formal elimination of the 20 triangle-capped Pd(G) atoms and attached P(G) atoms in shell 4 of **3** together with formal attachment of 30 P(F) atoms to the 30 square-capped Pd(F) atoms of **2**. [Panel b reprinted with permission from ref 14b. Copyright 2007 American Chemical Society.]

determined for shells 1 and 2 in the recently reported Au₁₃₃ nanocluster (**4**).^{20,21}

The icosahedral two-shell Pd architecture of **1** (Figure 1) shows that the 55 Pd atoms in **1** correspond to the two-shell icosahedral Mackay “hard-sphere” model.¹ Figure 2a discloses that each of the 20 triply bridging CO groups shown in Figure 1 is symmetrically linked to the centered Pd(D)₃ triangle of each 6-atom ν_2 triangular Pd(C)₃Pd(D)₃ face of the ν_2 icosahedral second shell. The 12 PR₃ ligands are expectedly attached to the

Table 1. Comparative Mean Metal-Metal Distances (with Atom Labels Given in Figure 2a) for Two-Shell Pd₅₅{P(*i*-Pr)₃}₁₂(μ₃-CO)₂₀ (1) in 1a Versus Those for Interior Icosahedral Shells 1 and 2 in PtPd₁₆₄ Cluster 3, in Pd₁₄₅ Cluster 2, and in Au₁₃₃ Cluster 4

connectivity ^a	N ^b	distance (Å)				
		1a ^c	3 ^d	2 ^e	4 ^f	Δ(4 - 2) ^g
M(A)-M(B)	12	2.63	2.64	2.63	2.76	+0.13
M(B)-M(B)	30	2.76	2.78	2.77	2.90	+0.13
M(B)-M(C)	12	2.64	2.73	2.74	2.81	+0.07
M(B)-M(D)	60	2.79	2.73	2.70	2.83	+0.13
M(C)-M(D)	60	2.77	2.83	2.82	2.93	+0.11
M(D)-M(D)	60	2.88	2.84	2.82	2.96	+0.14

^aM(A) designates central metal atom in each cluster. ^bN denotes number of individual distances under pseudo-*I_h* symmetry. ^cBased upon crystal-solvated Pd₅₅ cluster 1 in 1a possessing C₂(I) site symmetry that corresponds to 28 crystallographically independent Pd atoms with 27 Pd atoms encompassing the central Pd atom lying on the inversion center. ^dCrystallographically independent unit of PtPd₁₆₄ cluster 3 composed of 12 metal atoms of cubic *T_h*(2/*m* $\bar{3}$) site symmetry. ^eCrystallographically independent unit of Pd₁₄₅ cluster 2 composed of 25 Pd atoms of trigonal *S₆*($\bar{3}$) site symmetry. ^fCrystallographically independent unit of Au₁₃₃ cluster 4 composed of 69 Au atoms of monoclinic *C₂* site symmetry. ^gΔ(4 - 2) denotes difference between corresponding mean distances (Å) of Au in 4 and of Pd in 2; the difference in bulk metal-metal distance between ccp Au metal (2.884 Å) and ccp Pd metal (2.751 Å) at 20 °C is +0.13 Å.²⁴

Pd(C) atoms in the second shell. Table 1 shows that the corresponding values for each of the two types of metal-metal distances in shell 1 are essentially the same as those in 2 and 3, whereas corresponding mean distances for each of the four types of metal-metal distances in shell 2 differ markedly from those in 2 and 3. In 1, the two mean radial M(A)-Pd(B) and Pd(B)-Pd(C) distances, 2.63 and 2.64 Å in shells 1 and 2, respectively, are virtually identical, while in the second shell of 2 and 3 the mean Pd(B)-Pd(C) distances, 2.74 and 2.73 Å, respectively, are 0.1 Å longer. Similarly, in 1 the tangential mean Pd(C)-Pd(D) distance of 2.77 Å in shell 2 is 0.05 Å shorter than the corresponding tangential mean distances of 2.82 and 2.83 Å in shell 2 for 2 and 3, respectively. The icosahedral geometry of 1 expectedly imposes an analogous uniform contraction of the *radial* metal-metal edges versus the *tangential* metal-metal edges in 1, as previously found for both 2 and 3, namely, [(2.76 - 2.63 Å)/2.63 Å] × 100 = 4.9% for shell 1 and [(2.76 + 2.77 Å) - (2.63 + 2.64 Å)/(2.63 + 2.64 Å)] × 100 = 4.9% for combined shells 1 and 2; these identical values for the determined *radial* edge compressions versus polyhedral *tangential* edges in 1 are in complete agreement with the value of ~5% predicted by Mackay¹ based upon angular strain considerations. In contrast, for regular *ccp/hcp* metal arrangements (including the proposed Schmid cuboctahedral models⁵), all metal-metal distances are equivalent.

The large tangential mean Pd(D)-Pd(D) distance of 2.88 Å in the central Pd(D)₃ triangle of the 6-atom triangular Pd(C)₃Pd(D)₃ face in 1, which is 0.1 Å longer than the other mean Pd-Pd distances in 1 and 0.06, 0.04 Å longer than the corresponding mean Pd(D)-Pd(D) distances in 2 and 3, respectively, is attributed to the presumed extensive occurrence of d_π(Pd)-π*(CO) backbonding from the Pd(D) atoms to the symmetrically attached triply bridging CO group in 1 (Figure 2a). This premise is not only consistent with mean identical C-O bond lengths of 1.17 Å in 1a [range 1.16(1)–1.18(1) Å] and in 1b [range 1.15(1)–1.17(1) Å] but also in accordance with the low IR single

carbonyl frequency of ~1750 cm⁻¹ in paratone (Figure S5). This highly distinguishable IR frequency has been invaluable in the isolation of this cluster.

The two identical mean Pd(C)-P(C) distances for the six crystallographically independent P(*i*-Pr)₃ ligands of 2.24 Å in 1a [range 2.236(2)–2.247(2) Å] and 1b [range 2.233(3)–2.246(3) Å] are significantly shorter than the mean Pd-P distances of 2.32 Å for 2 (with 30 PEt₃) and 2.29 Å for 3 (with 20 PPh₃). Identical mean Pd-PEt₃ distances of 2.33 Å were found for the isostructural but non-isovalent bicuboctahedral Pd₃₀(CO)₂₆(PEt₃)₁₀^{25a} and Au₂Pd₂₈(CO)₂₆(PEt₃)₁₀.^{25b} These considerably shorter mean Pd-PPR₃ distances in 1 are likely due to unusually strong Pd(C)-PPR₃ σ-bonding with PPR₃. The single peak in the ³¹P{¹H} NMR spectrum of 1 at 57.26 ppm (external std. H₃PO₄) in CDCl₃ (Figure S6) is consistent with its pseudo-*I_h* symmetry.

Single-point DFT calculations, similar to previously performed computational analyses of other nanosized Pd clusters,^{25b} were likewise carried out via the Gaussian 09 computational package.²⁶ The hybrid gradient-corrected (generalized gradient approximation, GGA) DFT functional B3PW91, which combines the Becke three-fitted parametrization scheme^{27a} with a nonlocal PW91 correlation scheme,^{27b} was utilized. The modified scalar-relativistic effective core potential (ECP) basis set (LANL2DZ) of Hay and Wadt^{27c} was employed for Pd atoms. It includes the LANL2 ECP treatment of core electrons^{27c} with an explicit treatment of the outermost core and valence electrons. The modification was comprised of re-optimization of outer p-functions as described in ref 27d. P atoms were treated with standard LANL2DZ basis set augmented with an extra 3d polarization function (with exponent 0.364).^{27e} The Pople 6-31G* all-electron basis set^{27f} was used for C, O, and H atoms. Natural population analysis (NPA) was performed by use of the NBO software package (ver. 5.9) as implemented in Gaussian 09.^{27g,h} A high positively charged Pd₄₂ surface of +1.93 *e* (+0.046 *e* per atom) was displayed relative to the negatively charged *inner* Pd₁₂ shell of -0.89 *e* (-0.074 *e* per atom) and central Pd atom (-0.245 *e*). This charge distribution reflects combined negative-charged effects of the *inner* Pd₁₃ core of 1 and dominant *ligand* dπ(Pd)-π*(CO) backbonding. The overall negative *ligand* charge of -0.84 *e* is the result of the fact that the total negative charge of -2.40 *e* on 20 CO ligands is only partially balanced by electron depletion of total charge of +1.56 *e* on 12 PH₃ ligands.

Particularly noteworthy is the recently reported crystal structure determination²⁸ of a barrel-shaped chiral Au₁₃₀-(SC₆H₄-*p*-Me)₅₀ nanocluster that is geometrically related to the icosahedral Au₁₃₃ nanocluster. Its inner 55 Au atoms are organized into a 5-fold twinned two-shell decahedron²⁹ (instead of the interior 20-fold twinned Au₅₅ icosahedron found in the Au₁₃₃ nanocluster). The resulting three-shell quasi-*D_{5h}* Au₁₀₅ pentagonal kernel with shell 4 comprised of 25 monomeric RS-Au-SR staples possessing a different surface-shell pattern emphasizes the extremely important role played by the different thiolate ligands in determining the size and structure of gold nanoclusters.

Due to relatively weak metal-metal bonding in the above-mentioned icosahedral metal clusters, their stabilities are ensured by the presence of *bridging* (multidentate) ligands. Such ligands are either “staple”-like Au_{*n*}(RS)_{*n*+1}⁻ units in gold clusters or simply bridging carbonyl ligands in the case of transition metal carbonyl clusters. Metal-metal bonding alone involving late transition metals cannot substantially stabilize close-packed assemblies of large metal cluster units without assistance from generally stronger metal-ligand interactions. The importance of

bridging carbonyl ligands in stabilizing this nanosized close-packed metal cluster suggests (in accordance with the DFT calculations) extensive metal-to-CO electron transfer due to dominant $d\pi(\text{Pd})-\pi^*(\text{CO})$ backbonding.

■ ASSOCIATED CONTENT

Supporting Information

The Supporting Information is available free of charge on the ACS Publications website at DOI: 10.1021/jacs.5b13076.

Experimental details and spectroscopic data, including Figures S1–S6 and Table S1 (PDF)

Crystallographic data for **1a** (CIF)

Crystallographic data for **1b** (CIF)

■ AUTHOR INFORMATION

Corresponding Author

*dahl@chem.wisc.edu

Present Address

‡J.D.E.: Judson University, Elgin, IL 60123, USA

Notes

The authors declare no competing financial interest.

■ ACKNOWLEDGMENTS

Dedicated to the memory of Lord Jack Lewis. This research was supported by the Chemistry Department and Graduate School (Hilldale Foundation, UW-Madison). We thank Prof. June Dahl (UW School of Medicine & Public Health) for helpful suggestions. This work was also partially performed at the Center for Integrated Nanotechnologies, an Office of Science User Facility operated for the U.S. Department of Energy Office of Science. Los Alamos National Laboratory, an affirmative action equal opportunity employer, is operated by Los Alamos National Security, LLC, for the National Nuclear Security Administration of the U.S. Department of Energy under contract DE-AC52-06NA25396.

■ REFERENCES

- Mackay, A. L. *Acta Crystallogr.* **1962**, *15*, 916.
- Alvarez, S. *Dalton Trans.* **2005**, 2209.
- Wenninger, M. J. *The Thirteen Semiregular Convex Polyhedra and Their Duals*. In *Dual Models*; Cambridge University Press: Cambridge, UK, 1983; Chap. 2, pp 14–35.
- Weisstein, E. W. *Semiregular Polyhedron*. *MathWorld*, A Wolfram Web Resource; <http://mathworld.wolfram.com/SemiregularPolyhedron.html>.
- (a) Schmid, G. *Chem. Rev.* **1992**, *92*, 1709 and references therein. (b) Schmid, G. In *Physics and Chemistry of Metal Cluster Compounds*; de Jongh, L. J., Ed.; Kluwer Academic Publ.: Dordrecht/Boston/London, 1994; Chap. 3, pp 107–134. (c) Schmid, G. In *Clusters and Colloids: From Theory to Applications*; Schmid, G., Ed.; VCH Publ. Inc.: New York, 1994; pp 178–211.
- (a) Echt, O.; Sattler, K.; Recknagel, E. *Phys. Rev. Lett.* **1981**, *47*, 1121. (b) Hoare, M. R. *Adv. Chem. Phys.* **1979**, *40*, 49.
- Kuo, K. H. *Struct. Chem.* **2002**, *13*, 221.
- Elser, V.; Henley, C. L. *Phys. Rev. Lett.* **1985**, *55*, 2883.
- Guyot, P.; Audier, M. *Philos. Mag. B* **1985**, *52*, L15.
- (a) Shechtman, D.; Blech, I.; Gratias, D.; Cahn, J. W. *Phys. Rev. Lett.* **1984**, *53*, 1951. (b) Shechtman, D. Nobel Lecture: Quasi-Periodic Materials - A Paradigm Shift in Crystallography, 2011; http://www.nobelprize.org/nobel_prizes/chemistry/laureates/2011/shechtman-lecture.html
- Levine, D.; Steinhardt, P. J. *Phys. Rev. Lett.* **1984**, *53*, 2477.
- Henley, C. L. *Comments Cond. Matter Phys.* **1987**, *13*, 59.
- (a) Mednikov, E. G.; Dahl, L. F. *Philos. Trans. R. Soc., A* **2010**, 368, 1301. (b) Mednikov, E. G.; Dahl, L. F. *J. Chem. Educ.* **2009**, *86*, 1135.
- (a) Tran, N.; Powell, D.; Dahl, L. F. *Angew. Chem., Int. Ed.* **2000**, *39*, 4121. (b) Mednikov, E. G.; Jewell, M.; Dahl, L. F. *J. Am. Chem. Soc.* **2007**, *129*, 11619.
- Jennison, D. R.; Schultz, P. A.; Sears, M. P. *J. Chem. Phys.* **1997**, *106*, 1856.
- Northby, J. A. *J. Chem. Phys.* **1987**, *87*, 6166.
- (a) Wales, D.; Munro, L.; Doye, J. J. *Chem. Soc., Dalton Trans.* **1996**, 611. (b) Wales, D.; Doye, J. J. *Phys. Chem. A* **1997**, *101*, 5111. (c) Doye, J. P. K.; Wales, D. J. *J. Chem. Soc., Faraday Trans.* **1997**, *93*, 4233.
- (a) Farges, J.; de Feraudy, M. F.; Raoult, B.; Torchet, G. *J. Chem. Phys.* **1986**, *84*, 3491. (b) Farges, J.; de Feraudy, M. F.; Raoult, B.; Torchet, G. *Adv. Chem. Phys.* **1988**, *70*, 45.
- (a) Kroto, H. W.; Heath, J. R.; O'Brien, S. C.; Curl, R. F.; Smalley, R. E. *Nature* **1985**, *318*, 162. (b) Krätschmer, W.; Lamb, L. D.; Fostiropoulos, K.; Huffman, D. R. *Nature* **1990**, *347*, 354. (c) Hou, J. G.; Zhao, A. D.; Huang, T.; Lu, S. In *Encyclopedia of Nanoscience and Nanotechnology*; Nalwa, H. S., Ed.; American Scientific Publishers: Valencia, CA, 2004; Vol.1, pp 404–474.
- Dass, A.; Theivendran, S.; Nimmala, P. R.; Kumara, C.; Jupally, V. R.; Fortunelli, A.; Sementa, L.; Barcaro, G.; Zuo, X.; Noll, B. C. *J. Am. Chem. Soc.* **2015**, *137*, 4610.
- (a) Zeng, C.; Chen, Y.; Kirschbaum, K.; Appavoo, K.; Sfeir, M. Y.; Jin, R. *Sci. Adv.* **2015**, *1*, e1500045. (b) Kirschbaum, K.; Zeng, C.; Chen, Y.; Appavoo, K.; Sfeir, M. Y.; Jin, R. Poster presented at the 65th American Crystallographic Association Meeting, Philadelphia, PA, July 25–29, 2015.
- $\text{Pd}_{55}(\text{CO})_{20}(\text{PPR}^i_3)_{12}(\text{i-Pr})_2\text{O}$: $\text{C}_{134}\text{H}_{266}\text{O}_{21}\text{Pd}_{55}$, $M = 8437.11$, Cu $K\alpha$ wavelength; monoclinic, $P2_1/n$; $Z = 2$; $a = 19.1528(7)$ Å, $b = 25.4979(9)$ Å, $c = 19.9070(7)$ Å, $\alpha = \gamma = 90^\circ$, $\beta = 93.430(2)^\circ$; $V = 9704.3(6)$ Å³; $d(\text{calc}) = 2.887$ Mg/m³; $F(000) = 7896$. Full-matrix least-squares refinement on 18 754 independent merged ($R(\text{int}) = 0.0575$) reflections (1022 parameters, 20 restraints) converged at $wR_2(F^2) = 0.1053$ for all data; $R_1(F) = 0.0361$ for $I > 2\sigma(I)$; GOF on $F^2 = 1.033$; max/min residual electron density, $2.18/-3.79$ e·Å⁻³. The Pd_{55} molecule lies on a crystallographic inversion center. CCDC deposition number 1440303; CIF file available as SI.
- $\text{Pd}_{55}(\text{CO})_{20}(\text{PPR}^i_3)_{12}\cdot 5.5\text{THF}$: $\text{C}_{150}\text{H}_{296}\text{O}_{25.5}\text{Pd}_{55}$, $M = 8731.51$, Mo $K\alpha$ wavelength; monoclinic, $C2/c$; $Z = 4$; $a = 31.0979(7)$ Å, $b = 20.9092(5)$ Å, $c = 32.2003(7)$ Å, $\alpha = \gamma = 90^\circ$, $\beta = 98.119(1)^\circ$; $V = 20723.7(8)$ Å³; $d(\text{calc}) = 2.799$ Mg/m³; $F(000) = 16440$. Full-matrix least-squares refinement on 25 748 independent merged ($R(\text{int}) = 0.0463$) reflections (952 parameters, 81 restraints) converged at $wR_2(F^2) = 0.1285$ for all data; $R_1(F) = 0.0442$ for $I > 2\sigma(I)$; GOF on $F^2 = 1.075$; max/min residual electron density, $2.23/-3.01$ e·Å⁻³. The Pd_{55} molecule lies on a crystallographic 2-fold axis. CCDC deposition number 1440302; CIF file available as SI.
- Donohue, J. *The Structures of the Elements*; John Wiley & Sons: New York, 1974.
- (a) Mednikov, E. G.; Ivanov, S. A.; Dahl, L. F. *Angew. Chem., Int. Ed.* **2003**, *42*, 323. (b) Mednikov, E. G.; Ivanov, S. A.; Dahl, L. F. *Inorg. Chem.* **2011**, *50*, 11795.
- Frisch, M. J.; et al. *Gaussian 09*, revision A.1; Gaussian, Inc.: Wallingford, CT, 2009.
- (a) Becke, A. D. *J. Chem. Phys.* **1993**, *98*, 5648. (b) Perdew, J. P.; Burke, K.; Wang, Y. *Phys. Rev. B: Condens. Matter Mater. Phys.* **1996**, *54*, 16533. (c) Hay, P. J.; Wadt, W. R. *J. Chem. Phys.* **1985**, *82*, 270; **1985**, *82*, 299. (d) Couty, M.; Hall, M. B. *J. Comput. Chem.* **1996**, *17*, 1359. (e) Check, C. E.; Faust, T. O.; Bailey, J. M.; Wright, B. J.; Gilbert, T. M.; Sunderlin, L. S. *J. Phys. Chem. A* **2001**, *105*, 8111. (f) Hariharan, P. C.; Pople, J. A. *Theor. Chim. Acta* **1973**, *28*, 213. (g) Reed, A. E.; Weinstock, R. B.; Weinhold, F. *J. Chem. Phys.* **1985**, *83*, 735. (h) Weinhold, F.; Landis, C. R. *Valency and Bonding: A Natural Bond Orbital Donor-Acceptor Perspective*; Cambridge University Press: Cambridge, UK, 2005.
- Chen, Y.; Zeng, C.; Liu, C.; Kirschbaum, K.; Gayathri, C.; Gil, R. R.; Rosi, N. L.; Jin, R. *J. Am. Chem. Soc.* **2015**, *137*, 10076.
- Ino, S. *J. Phys. Soc. Jpn.* **1969**, *27*, 941.